The Plant Cell, Vol. 31: 699–714, March 2019, www.plantcell.org © 2019 ASPB.

The Transcription Factor MYB59 Regulates K^+/NO_3^- Translocation in the Arabidopsis Response to Low K^+ Stress[OPEN]

Xin-Qiao Du,[a,1] Feng-Liu Wang,[a,1] Hong Li,[a] Si Jing,[a] Miao Yu,[a] Jigang Li,[a] Wei-Hua Wu,[a] Jörg Kudla,[a,b] and Yi Wang[a,2]

[a] State Key Laboratory of Plant Physiology and Biochemistry, College of Biological Sciences, China Agricultural University, Beijing 100193, China

[b] Institut für Biologie und Biotechnologie der Pflanzen, Universität Münster, 48149 Münster, Germany

ORCID IDs: 0000-0001-7162-9242 (X.-Q.D.); 0000-0002-0831-523X (F.-L.W.); 0000-0002-7629-9315 (H.L.); 0000-0001-9774-4329 (S.J.); 0000-0002-5972-5431 (M.Y.); 0000-0002-4395-2656 (J.L.); 0000-0002-0642-5523 (W.-H.W.); 0000-0002-8238-767X (J.K.); 0000-0002-3660-5859 (Y.W.)

Potassium and nitrogen are essential nutrients for plant growth and development. Plants can sense potassium nitrate (K^+/NO_3^-) levels in soils, and accordingly they adjust root-to-shoot K^+/NO_3^- transport to balance the distribution of these ions between roots and shoots. In this study, we show that the transcription factorMYB59 maintains this balance by regulating the transcription of the Arabidopsis (*Arabidopsis thaliana*) *Nitrate Transporter1.5* (*NRT1.5*)/ *Nitrate Transporter/Peptide Transporter Family7.3* (*NPF7.3*) in response to low K^+ (LK) stress. The *myb59* mutant showed a yellow-shoot sensitive phenotype when grown on LK medium. Both the transcript and protein levels of *NPF7.3* were remarkably reduced in the *myb59* mutant. LK stress repressed transcript levels of both *MYB59* and *NPF7.3*. The *npf7.3* and *myb59* mutants, as well as the *npf7.3 myb59* double mutant, showed similar LK-sensitive phenotypes. Ion content analyses indicated that root-to-shoot K^+/NO_3^- transport was significantly reduced in these mutants under LK conditions. Moreover, chromatin immunoprecipitation and electrophoresis mobility shift assay assays confirmed that MYB59 bound directly to the *NPF7.3* promoter. Expression of *NPF7.3* in root vasculature driven by the *PHOSPHATE 1* promoter rescued the sensitive phenotype of both *npf7.3* and *myb59* mutants. Together, these data demonstrate that *MYB59* responds to LK stress and directs root-to-shoot K^+/NO_3^- transport by regulating the expression of *NPF7.3* in Arabidopsis roots.

INTRODUCTION

Potassium (K) and nitrogen (N) are essential macronutrients for plant growth and development. In plants, K^+ is the most abundant cation, which constitutes 2% to 10% of the plant's dry weight (Leigh and Wyn Jones, 1984). Its functions include enzyme activation, osmotic regulation, and electrical neutralization (Clarkson and Hanson, 1980). Besides, it can facilitate photosynthesis, starch synthesis, and transport of assimilation products (Pettigrew, 2008; Zörb et al., 2014). Nitrogen is the macronutrient that plants require in the greatest amounts. It is part of numerous organic compounds and is an essential component of amino acids, proteins, and nucleic acids (Mengel and Kirkby, 2001). Therefore, sufficient K and N supplies are necessary to promote crop yield and quality, as well as to enhance crop resistance to biotic and abiotic stresses.

For most terrestrial plants, K^+ and nitrate (NO_3^-) are the major forms of potassium and nitrogen that are absorbed by plant roots and transported within plants. They represent the most abundant inorganic cation and anion, respectively, in plant cells, and their absorption and transport have to be coordinated (Blevins et al., 1978; Triplett et al., 1980; White, 2012) for proper growth and development. However, in agricultural production, excessive application of nitrogen fertilizer with insufficient potassium fertilizer disturbs the N/K balance. This reduces the efficiency of fertilizer utilization and results in environmental pollution (Guo et al., 2010; Zhang, 2017). Therefore, understanding the mechanisms that coordinate N and K uptake and transport is critical for both the improvement of crop nutrient efficiency and protection of our environment from excess fertilizer runoff.

K^+ and NO_3^- are absorbed into plant root cells by K^+ transporters and NO_3^- transporters, respectively. In Arabidopsis (*Arabidopsis thaliana*), the K^+ channel ARABIDOPSIS K^+ TRANSPORTER1 and the K^+ transporters HIGH AFFINITY K^+ TRANSPORTER5 (HAK5) and K^+ UPTAKE PERMEASE7 (KUP7) are major components involved in K^+ uptake (Hirsch et al., 1998; Rubio et al., 2000; Gierth et al., 2005; Pyo et al., 2010; Adams and Shin, 2014; Han et al., 2016). The absorption of NO_3^- is mediated by transporters of the Nitrate Transporter 1/Peptide Transporter (NRT1/PTR) and NRT2 families (Chen et al., 2008; Wang et al., 2012; Léran et al., 2014; O'Brien et al., 2016). After absorption into root cells, K^+ and NO_3^- are released into xylem vessels and subsequently transported toward the shoot. In Arabidopsis, the K^+ channel STELAR K^+ OUTWARD RECTIFIER (SKOR) and the K^+ transporter KUP7 are responsible for

[1] These authors contributed equally to this work.
[2] Address correspondence to yiwang@cau.edu.cn.
The author responsible for distribution of materials integral to the findings presented in this article in accordance with the policy described in the Instructions for Authors (www.plantcell.org) is: Yi Wang (yiwang@cau.edu.cn).
[OPEN]Articles can be viewed without a subscription.
www.plantcell.org/cgi/doi/10.1105/tpc.18.00674

root-to-shoot K^+ transport (Gaymard et al., 1998). The NO_3^- transporter NRT1.5 is involved in root-to-shoot NO_3^- transport (Lin et al., 2008), and is now known asNitrate Transporter/Peptide Transporter Family 7.3 (NPF7.3, in the NRT1/PTR family; Léran et al., 2014). Our recent study revealed that NPF7.3 can also function as a proton-coupled H^+/K^+ antiporter, which also mediates root-to-shoot K^+ translocation (Li et al., 2017). Therefore, NPF7.3 plays essential roles in regulating the coordinated transport of K^+/NO_3^- from root to shoot in Arabidopsis (Lin et al., 2008; Drechsler et al., 2015; Meng et al., 2016; Li et al., 2017).

Plants can sense K^+/NO_3^- levels in soils, and accordingly can regulate K^+/NO_3^- uptake as well as root-to-shoot translocation to balance the distribution of these ions between roots and shoots. Under nutrient sufficient conditions, the root-to-shoot K^+/NO_3^- transport is enhanced. Conversely, this transport is restricted in plants under nutrient-limited conditions. Previous studies have revealed that *SKOR* and *NPF7.3* are regulated at the transcriptional level in response to external K^+/NO_3^- levels. The transcripts of both *SKOR* and *NPF7.3* are upregulated by the NO_3^- supply (Wang et al., 2004; Lin et al., 2008). During low K^+ stress, the *NPF7.3* transcript is downregulated to inhibit root-to-shoot K^+/NO_3^- transport (Lin et al., 2008; Li et al., 2017). It has been suggested that the coordination of root-to-shoot K^+/NO_3^- transport may be achieved via the transcriptional regulation of *SKOR* and *NPF7.3*. However, the underlying molecular mechanisms have remained unclear.

MYB-type transcription factors are members of a large family of important regulators in plants. There are ~339 and 230 MYB proteins in Arabidopsis and rice, respectively (Feller et al., 2011). They play crucial roles in various physiological processes (Dubos et al., 2010) such as hormone response (Li et al., 2009; Peng, 2009), abiotic stress tolerance (Agarwal et al., 2006; Jung et al., 2008), plant development (Baumann et al., 2007; Wang et al., 2009; Zhang et al., 2013), and metabolic regulation (Zhong et al., 2008; Zhou et al., 2009). Here, we showed that the MYB transcription factor MYB59 directly bound to the *NPF7.3* promoter and positively regulated expression of the *NPF7.3* transcript in Arabidopsis in response to external K^+/NO_3^- levels. *MYB59* and *NPF7.3* function in same pathway to coordinate root-to-shoot K^+/NO_3^- transport.

RESULTS

Arabidopsis myb59 Mutants Are Sensitive to Low K^+ Stress

To identify important components involved in the response to low K^+, over 400 Arabidopsis T-DNA insertion mutants were analyzed for potential low K^+ phenotypes. Among these mutants, the MYB transcription factor mutant *myb59-1* showed a very sensitive phenotype on low K^+ (LK; 100 μM K^+) medium (Figure 1A; Supplemental Figure 1A). When seedlings were grown on LK medium for 10 d, shoots of *myb59-1* became yellow (a typical symptom of K^+ deficiency), whereas the wild-type shoots remained green (Figure 1A). Under high K^+ (HK; 5 mM K^+) conditions, there was no phenotypic difference between wild-type and mutant plants (Figure 1A). *MYB59* can produce four distinctively spliced transcripts (*MYB59.1* to *MYB59.4*), and *MYB59.4* appears to have no known function (Li et al., 2006). The other three transcripts are all disrupted in the *myb59-1* mutant (Figures 1B and 1C). A CRISPR/Cas9 mutant of *MYB59* (*myb59-2*) was constructed and displayed a similar low K^+-sensitive phenotype as seen with *myb59-1* (Figures 1A and 1D). Complementation lines of *myb59-1* (COM1 and COM2) generated by transformation with the genomic sequence of *MYB59* rescued the sensitive phenotype of *myb59-1* (Figures 1A and 1C). These data suggested that the transcription factor MYB59 is involved in the low K^+ response. The transcript levels of *MYB59* in all these plants were analyzed and are shown in Figures 1C and 1E.

MYB59.3 encodes an R2R3 (Repeat2 Repeat3) transcription factor MYB59.3 that contains two amino acid sequence repeats R2 and R3 in the N terminus (Dubos et al., 2010), whereas MYB59.1 and MYB59.2 have a truncated N terminus (Figure 1B). All three proteins mediated transcriptional activation activities in yeast (Figure 2A). To test their functions in planta, the coding sequences of each of the three transcripts driven by the native promoter were transformed into *myb59-1*, respectively. Phenotypic analyses showed that only the longest transcript (*MYB59.3*) could restore the phenotype of *myb59-1* to wild type (Figure 2B). The expression levels of the three transcripts are shown in Figure 2C. In addition, overexpression of *MYB59.3* in *myb59-1* (*myb59-1*/*ProSuper:MYB59.3-FLAG*) also complemented the low K^+ sensitive phenotype, but did not lead to an enhanced tolerance phenotype (Supplemental Figure 2). These results suggested that *MYB59.3* is the functional form in plants.

Root-to-Shoot K^+ Transport Is Reduced in *myb59* Mutants

Direct K^+ measurements indicated that, under LK conditions, the roots of *myb59* mutants accumulated more K^+ ions than roots of wild-type plants (Figure 3A). In contrast, the K^+ content in mutant shoots was significantly reduced, resulting in the low K^+ sensitive phenotype of *myb59* mutants (Figure 1A). The increased root/shoot ratios of K^+ in *myb59* mutants suggested that *MYB59* is involved in root-to-shoot K^+ transport under LK conditions (Figure 3B). In addition, the K^+ concentrations in the xylem exudates of mutant plants were significantly reduced under LK conditions (Figure 3C), further confirming the role of *MYB59* in root-to-shoot K^+ transport.

We observed that, although the K^+ content in *myb59* shoots was also slightly reduced on HK medium (Figure 3A), the K^+ concentrations in the xylem exudates of *myb59* mutants were not significantly changed under HK conditions (Figure 3C). This difference may be due to the different culture conditions used in the two experiments. For K^+ content measurement, plants were grown on sealed agar plates for 10 d. In contrast, for the K^+ concentration measurement of xylem exudates, plants were grown in vermiculite and irrigated with nutrient solution for 20 d. The differences in substrate, seedling age, and transpiration condition may influence K^+ translocation rate in xylem. In addition, nutrient solution has more freely diffusible K^+ ions compared with agar plates, which prevents the decreased K^+ concentration in mutant xylem.

Transcription of *NPF7.3* Is Reduced in *myb59* Mutants

To identify the target gene of MYB59, we conducted RNA-sequencing experiments to analyze the transcriptional changes

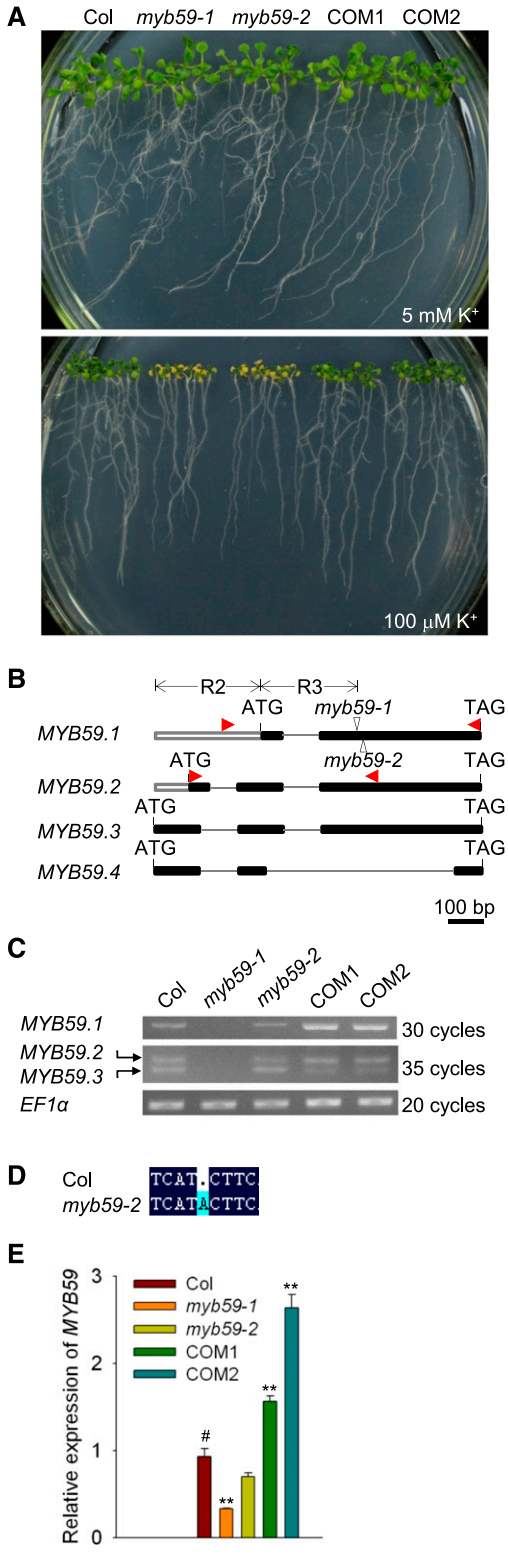

Figure 1. The *myb59* Mutant is Sensitive to Low K^+ Stress.

(A) Phenotypic comparison among wild-type plants (Col), two *myb59* mutants and two complementation lines (COM1 and COM2). Seedlings were germinated and grown on K^+-sufficient (5 mM) medium or low K^+ (100 μM) medium for 10 d.

(B) Schematic representation of four spliced transcripts of *MYB59*. The mutation sites are indicated by white triangles in *MYB59.1*. The red triangles show primer sites for the RT-PCR analysis described below. The two MYB domain repeats (R2 and R3) are indicated with sets of arrows.

(C) RT-PCR analysis of *MYB59* transcripts in various plants using the primer sites shown in **(B)**. *MYB59.1* was amplified using the top pair of primers; *MYB59.2* and *MYB59.3* were amplified using the bottom pair of primers. The *Elongation Factor (EF)1α* gene was used as an internal standard for normalization of gene expression levels.

(D) Partial alignment of the *myb59-2* mutant sequence with the wild-type sequence.

(E) RT-qPCR analysis of *MYB59* expression in various plants. RT-qPCR data are shown as means ± SE ($n = 3$ independent experiments as described in "Methods"). Student's *t* test (*$P < 0.05$ and **$P < 0.01$) was used to analyze statistical significance, and # represents control.

of K^+-related genes. Among these genes, the transcriptional levels of *HAK5* and *NPF7.3* were significantly reduced in *myb59* mutant plants under both MS (Murashige and Skoog) medium and LK conditions (Supplemental Table 1; Supplemental Figure 3A). *HAK5* functions in high-affinity K^+ uptake in Arabidopsis root (Gierth et al., 2005). It is considered to be a marker gene in the Arabidopsis response to K^+ deficiency, because its transcript level is strictly regulated by external K^+ levels (Gierth et al., 2005; Zhao et al., 2016). Previous studies reported that the transcription factors Related to AP2 11 and Auxin Response Factor 2 directly regulate *HAK5* expression (Kim et al., 2012; Zhao et al., 2016). In the present study, the high K^+ content in *myb59* mutant roots may impair or alleviate the K^+-deficiency signal and thereby could retard the induction of *HAK5* transcript in *myb59* mutants even under the low K^+ condition. $^{86}Rb^+$ uptake assays also suggested that the high-affinity K^+ uptake in *myb59* mutants was inhibited (Supplemental Figure 3B), and this was consistent with the reduced *HAK5* expression in *myb59* mutants (Supplemental Figure 3A). Phenotype tests indicated that *hak5* mutant plants did not show a similar sensitive phenotype like *myb59* under this low K^+ condition (Supplemental Figure 3C), suggesting that *HAK5* may not be a direct target of MYB59. However, the repressed *HAK5* transcription in *myb59* mutants may further enhance the low K^+ sensitive phenotype of *myb59* mutants.

NPF7.3 is involved in K^+ and NO_3^- translocation from root to shoot (Lin et al., 2008; Li et al., 2017). We found that the NO_3^- content in *myb59* mutant plants showed a similar pattern to the K^+ content (Figures 3D to 3F). Therefore, *MYB59* is also involved in root-to-shoot NO_3^- transport, especially under LK conditions, and this matches the physiological function of *NPF7.3*.

Both *NPF7.3* and *MYB59* are mainly expressed in Arabidopsis roots. *MYB59* transcripts could be detected in all root tissues and cell types. However, *NPF7.3* was specifically expressed in the root stele (Figure 4A). GUS staining and reverse transcription quantitative PCR (RT-qPCR) analyses confirmed that the level of the *NPF7.3* transcript was extremely low in roots of *myb59* mutants (Figures 4B and 4C). Disruption of *MYB59* also attenuated the level of NPF7.3 in the root stele (Figure 4D). These data suggested that *NPF7.3* is a target gene of MYB59.

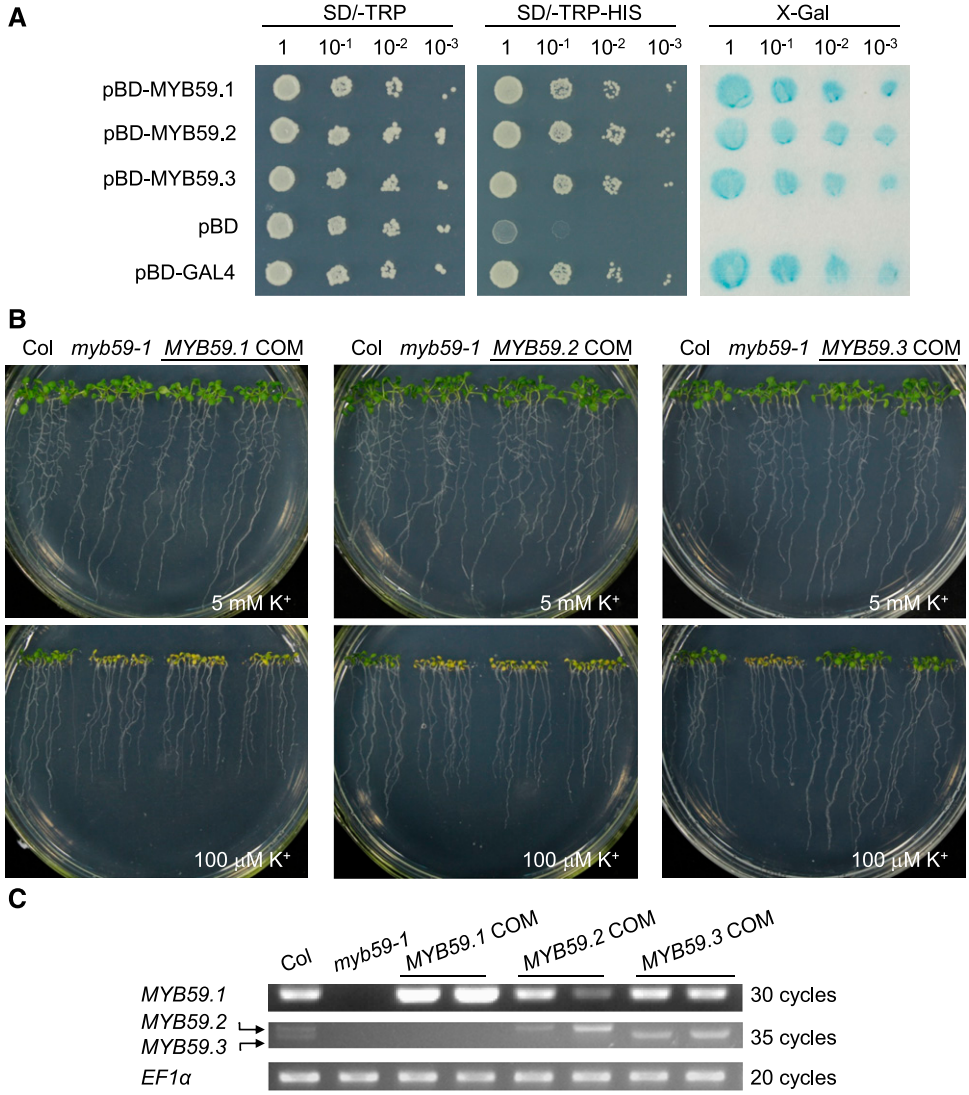

Figure 2. The *MYB59.3* is able to Rescue the Low K^+-Sensitive Phenotype of *myb59*.

(A) Transactivation resulting from the expression of three transcripts of *MYB59* in yeast as described in "Methods."pBD: empty vector that contains GAL4 DNA-binding domain. X-Gal: 5-Bromo-4-chloro-3-indolyl β-D-galactoside, which is used to test beta-galactosidase activity.
(B) Effect of K^+ concentration on growth phenotype. Wild-type plants, *myb59* mutant plants, and the complementation lines with three different *MYB59* transcripts (*MYB59.1* COM, *MYB59.2* COM, and *MYB59.3* COM) were grown in either 5 mM or 100 μM K^+ for 10 d.
(C) RT-PCR analysis of three *MYB59* transcripts in various plants. EF1α, elongation factor 1α.

SKOR is another important K^+ channel that mediates root-to-shoot K^+ transport (Gaymard et al., 1998). We also investigated whether *SKOR* is a target gene of MYB59. Based on the RNA-seq results, under the LK condition, we did not observe differences in *SKOR* expression between wild-type and *myb59* mutant plants (Supplemental Table 1). RT-qPCR results further confirmed that the *SKOR* transcript level was not altered in the *myb59* mutants (Supplemental Figure 4A). Moreover, a *SKOR* loss-of-function mutant (*skor*) did not display phenotypes that were comparable with *myb59* or *npf7.3* mutants (Supplemental Figure 4B). Together, these data indicated that *SKOR* is not a target gene of MYB59 in our experimental conditions.

Root-to-Shoot K^+/NO_3^- Transport Is Impaired in both *myb59* and *npf7.3* Mutants

Phenotype tests on LK medium showed that two allelic mutants of *NPF7.3* (*npf7.3* and *lks2*) displayed a very sensitive phenotype (yellow shoot) similar to *myb59* mutants (Figure 5A; Supplemental Figure 1B). In the *lks2* mutant, a single-nucleotide mutation resulted in a G209E substitution in NPF7.3 (Li et al., 2017). With increasing K^+ concentration in the medium, the yellow shoot phenotype of *npf7.3* and *myb59* gradually disappeared (Figure 5B). Because NPF7.3 is a key component mediating K^+ and NO_3^- translocation from root to shoot (Lin et al.,

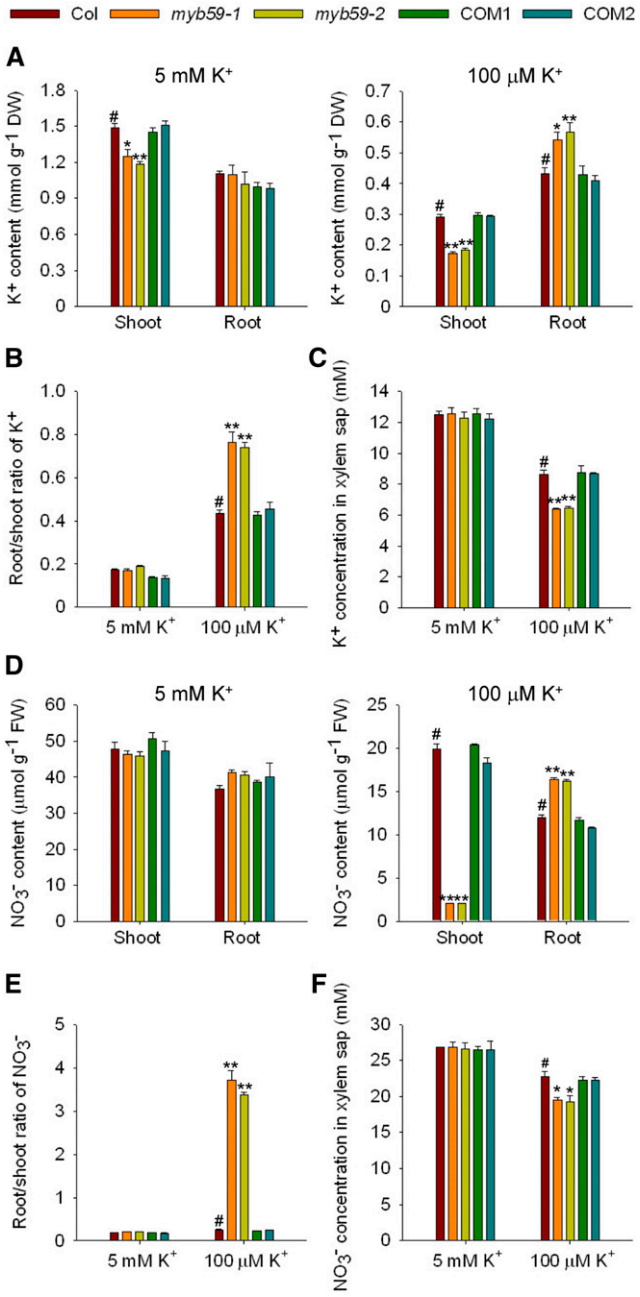

Figure 3. The *myb59* Mutant is Defective in Root-to-shoot Transport of K^+ and NO_3^-.

(A) and **(D)** K^+ and NO_3^- content measurement in various plant lines and organs after being germinated and grown on K^+-sufficient (5 mM) medium or low K^+ (100 μM) medium for 10 d.
(B) and **(E)** The root/shoot ratios of K^+ and NO_3^- per plant in various plant lines and organs.
(C) and **(F)** K^+ and NO_3^- concentrations in xylem exudates from *myb59* mutants and complementation lines after being cultured in solutions containing different K^+ concentrations (5 mM and 100 μM) for 20 d. Data in this figure are shown as means ±SE (n = 3 as described in "Methods"). Student's t test (*P < 0.05 and **P < 0.01) was used to analyze statistical significance, and # represents control.
DW, dry weight; FW, fresh weight.

2008; Li et al., 2017), the K^+ and NO_3^- contents in *npf7.3* and *myb59* mutants were determined. The results indicated that these two mutants displayed a very similar pattern regarding ion contents. Both *npf7.3* and *myb59* mutants had higher K^+ and NO_3^- contents in roots than wild-type plants under LK

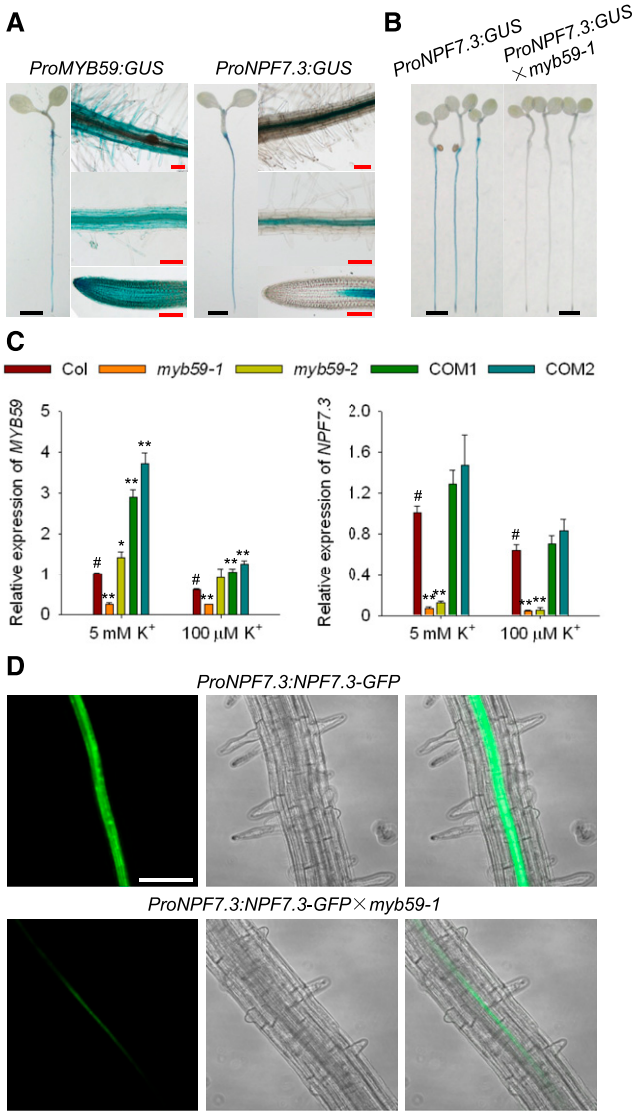

Figure 4. MYB59 Positively Regulates *NPF7.3* Expression.

(A) GUS staining of *ProMYB59:GUS* and *ProNPF7.3:GUS* transgenic plants. Bars in black = 1 mm, and bars in red = 100 μm.
(B) GUS staining showing expression of transcript *NPF7.3* in *myb59* mutant and wild-type plants. Bars = 1 mm.
(C) RT-qPCR analyses of *MYB59* and *NPF7.3* expression in *myb59* mutants and complementation lines. Seedlings were germinated and grown on K^+-sufficient (5 mM) medium or low K^+ (100 μM) medium for 8 d, and then roots were collected and used for RT-qPCR assays. RT-qPCR data are shown as means ±SE (n = 3 independent experiments as described in "Methods"). Student's t test (*P < 0.05 and **P < 0.01) was used to analyze statistical significance, and # represents control.
(D) Green fluorescent protein (GFP) fluorescence observation showing the expression of NPF7.3 in *myb59* mutant and wild-type plants. Bars = 100 μm.

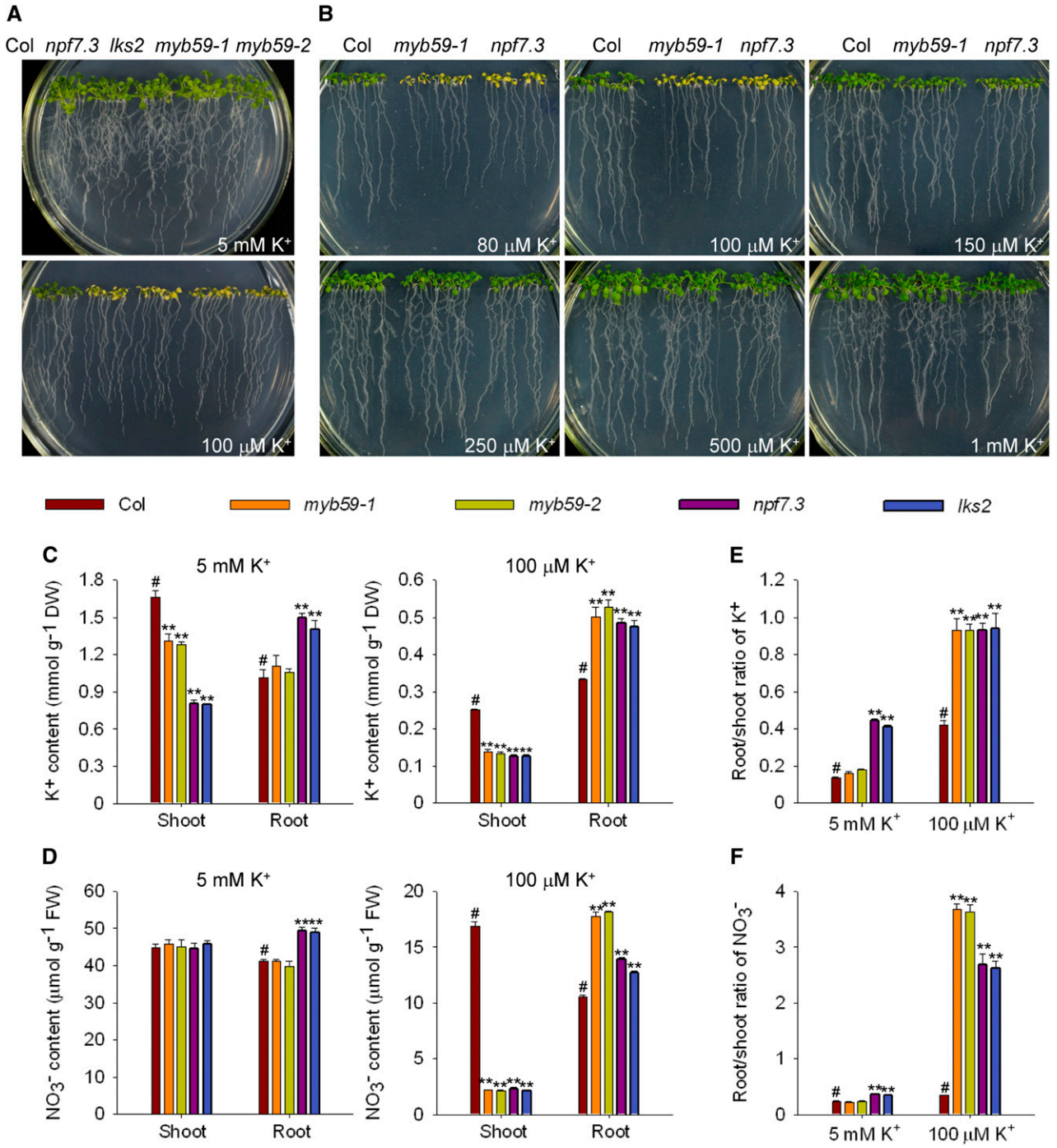

Figure 5. The *myb59* and *npf7.3* Show Similar Low K^+ Sensitive Phenotype.

(A) Effect of K^+ concentration on growth of *myb59*, *npf7.3*, and *lks2* mutants. The *lks2* is a single-nucleotide mutant of *NPF7.3*.
(B) Phenotypic analysis of *myb59* and *npf7.3* mutant plants after growth on medium containing different K^+ concentrations for 10 d.
(C) and **(D)** K^+ and NO_3^- content measurement in various plant lines and organs.
(E) and **(F)** The root/shoot ratios of K^+ and NO_3^- per plant in various plant materials. Data are shown as means ±SE ($n = 3$ as described in "Methods"). Student's *t* test (**P < 0.01) was used to analyze statistical significance, and # represents control.

conditions, whereas the K^+ and NO_3^- contents were significantly reduced in mutant shoots (Figures 5C and 5D). The root/shoot ratios indicated that root-to-shoot transport of both K^+ and NO_3^- is impaired in these mutants (Figures 5E and 5F).

We observed that the root/shoot ratios of NO_3^- in *npf7.3* and *myb59* mutants were more strongly affected than that of K^+ under LK conditions (Figures 5E and 5F). Besides NPF7.3, the K^+ channel SKOR and the K^+ transporter KUP7 also contribute to root-to-shoot K^+ translocation (Gaymard et al., 1998; Han et al., 2016). They are specific for K^+ transport, and do not transport NO_3^-. Importantly, the transcript levels of both *SKOR* and *KUP7* were not regulated by MYB59 (Supplemental Table 1; Supplemental Figure 4A). In contrast, NPF7.3 has been characterized as the major component for root-to-shoot NO_3^- transport (Lin et al., 2008; Li et al., 2017). Consistent with this, our results show a stronger effect of *myb59* and *npf7.3* mutants on the NO_3^- distribution than for K^+.

To determine whether *MYB59* and *NPF7.3* function in same pathway, a *myb59 npf7.3* double mutant was generated. Phenotype analyses and ion content measurements showed that the double mutant had both a similar sensitive phenotype and similar ion contents as the single mutants (Figures 6A and 6B; Supplemental Figure 1C). In addition, the K^+ concentrations in xylem sap in all these single and double mutants were lower than in wild-type plants under LK conditions, and were reduced to the same level (Figure 6C). These results indicated that *MYB59* and *NPF7.3* function in same regulatory

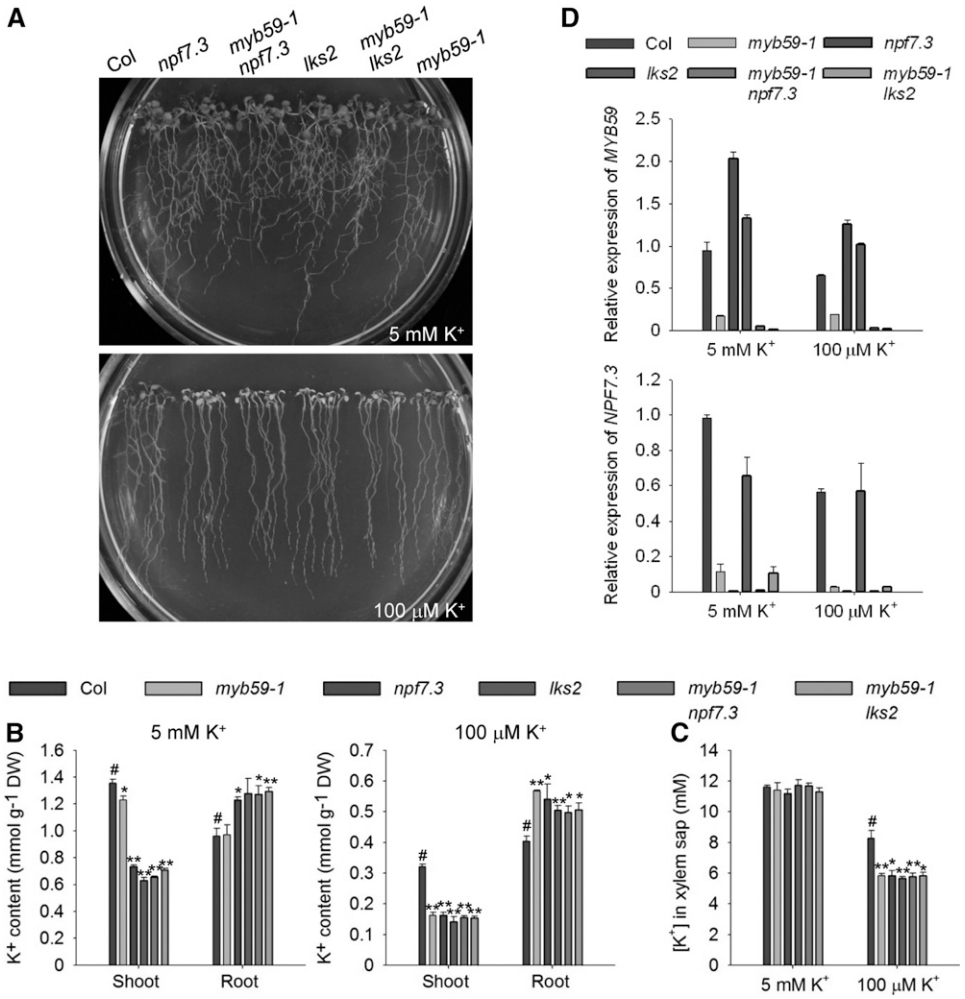

Figure 6. *MYB59* and *NPF7.3* Function in Same Pathway in Response to Low K^+ Stress.

(A) Effect of K^+ concentration on growth of single and double mutants of *myb59* and *npf7.3*.

(B) K^+ content measurement in various plant materials. DW, dry weight.

(C) K^+ concentrations in xylem exudates from various plants after being cultured in solutions containing different K^+ concentrations (5 mM and 100 μM) for 20 d. Data are shown as means ±SE ($n = 3$ as described in "Methods"). Student's *t* test (*$P < 0.05$ and **$P < 0.01$) was used to analyze statistical significance, and # represents control.

(D) RT-qPCR verification of *MYB59* and *NPF7.3* expression in various plants as indicated.

pathway. RT-qPCR results showed that the transcript levels of *NPF7.3* were remarkably reduced in both the *myb59* single mutant and the *myb59 lks2* double mutant, and *MYB59* transcripts were just slightly increased in *npf7.3* and *lks2* mutants (Figure 6D). These findings suggested that *NPF7.3* acts downstream of *MYB59*.

NPF7.3 Represents a Downstream Target Gene of MYB59

We performed genetic experiments to further address whether *NPF7.3* transcription is regulated by MYB59. A previous study reported that a *NPF7.3* coding sequence driven by a *PHO1* promoter could complement the phenotype of *npf7.3* mutant

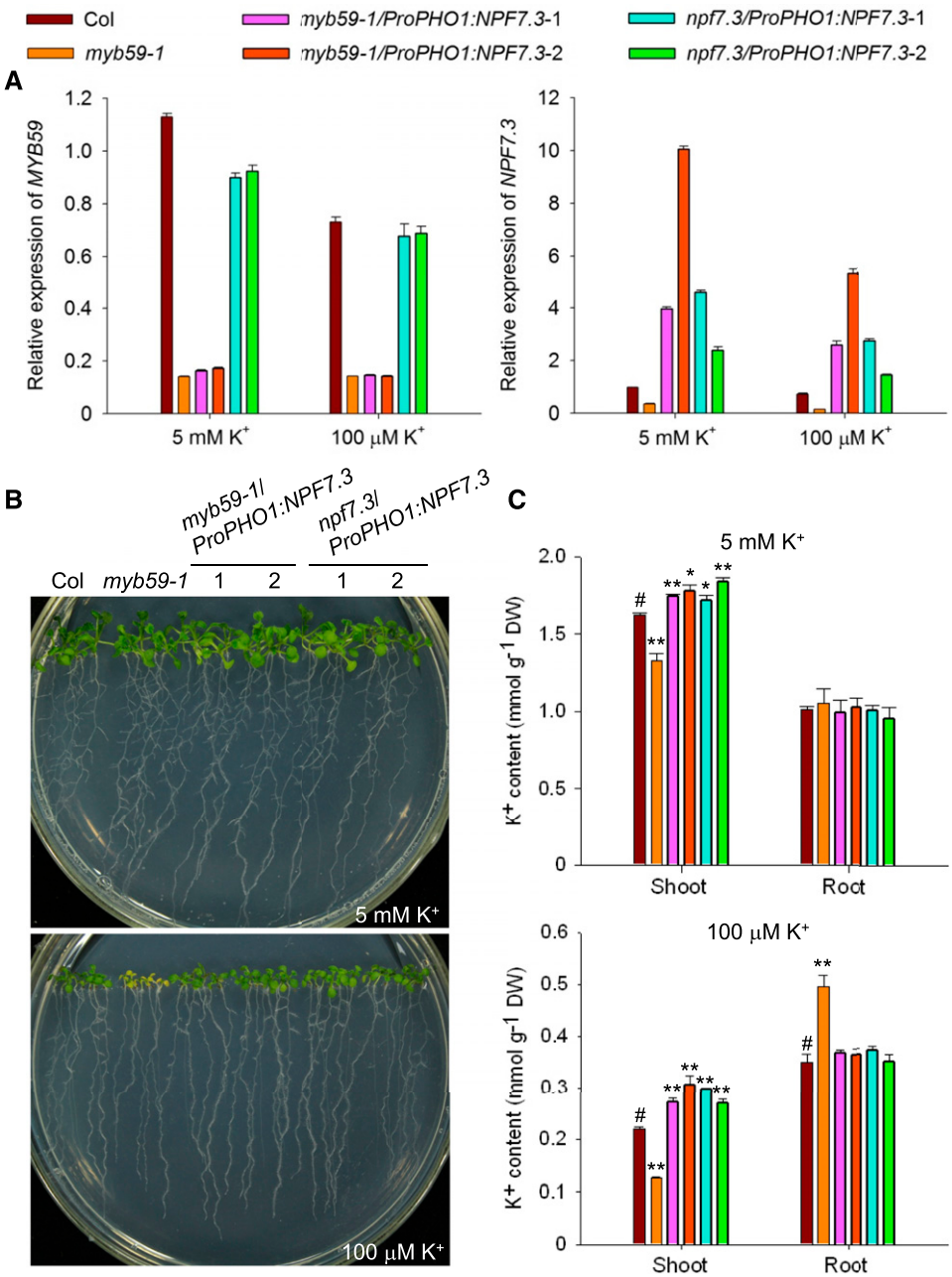

Figure 7. Genetic complementation of *myb59* Mutant by Expressing *NPF7.3* Under Control of the *PHO1* Promoter.

(A) RT-qPCR verification of *MYB59* and *NPF7.3* expression in various plants as indicated. RT-qPCR data are shown as means ±SE (*n* = 3 independent experiments as described in "Methods").

(B) Phenotype comparison among wild-type plants, *myb59* mutant, *myb59/ProPHO1: NPF7.3*, and *npf7.3/ProPHO1: NPF7.3* transgenic plants.

(C) K^+ content measurement in various plant materials. Data in **(C)** are shown as means ±SE (*n* = 3 biological replicates of xylem sap from 20-24 plants). Student's *t* test (*P < 0.05 and **P < 0.01) was used to analyze statistical significance, and # represents control. DW, dry weight.

(Drechsler et al., 2015). *PHO1* is involved in phosphate translocation from root to shoot, and its expression pattern in the root stele is similar to that of *NPF7.3* (Hamburger et al., 2002). *PHO1* transcript levels in *myb59* mutants were not significantly different (Supplemental Figure 3A). Therefore, we constructed the transgenic plants *npf7.3/ProPHO1:NPF7.3* and *myb59-1/ProPHO1:NPF7.3*. The *NPF7.3* transcripts were no longer reduced in these two transgenic plants (Figure 7A). Phenotype analyses showed that the *NPF7.3* genomic sequence driven by *PHO1* promoter could complement the low K^+ sensitive phenotype of both *npf7.3* and *myb59* mutants (Figure 7B; Supplemental Figure 1D; Supplemental Figure 5). The shoot K^+ contents in these transgenic plants were significantly increased, even to higher concentrations than that in wild-type plants (Figure 7C). These data clearly demonstrated that the low K^+ sensitive phenotype of *myb59* is due to reduction of *NPF7.3* transcription and identify *NPF7.3* as the downstream target gene of MYB59.

MYB59.3 Binds Directly to the *NPF7.3* Promoter

As a MYB-type transcription factor, MYB59 contains conserved R2R3 DNA binding domains at its N terminus that can bind to some *cis* elements (Mu et al., 2009; Prouse and Campbell, 2012). The *NPF7.3* promoter region contains some *cis* elements that may represent binding sites of MYB59. To determine whether MYB59 binds to the *NPF7.3* promoter, chromatin immunoprecipitation (ChIP) and electrophoresis mobility shift assay (EMSA) were performed. Because phenotype analyses indicated that only the transcript *MYB59.3* encodes the functional form of *MYB59* (Figure 2B), *myb59-1/ProSuper:MYB59.3-FLAG* transgenic plants were used for ChIP assays. Six DNA fragments (P1 to P6) within the *NPF7.3* promoter region (~1.6 kb) were studied (Figure 8A). Two fragments within *NPF7.3* exon regions were used as negative controls (Figure 8A). The ChIP results indicated that MYB59.3 could only bind to the P1 and P5 fragments (Figure 8B).

The DNA binding activity of MYB59 was also confirmed using EMSA. Both MYB59.3 and MYB59.1 (control) were fused with CTP:CMP-3-deoxy-D-mannooctulosonate cytidylyltransferase (CKS) protein and a His tag. The CKS-MYB59-His proteins were expressed in *Escherichia coli* and purified from the soluble fraction using an anti-His antibody. As shown in Figure 8C, MYB59.3 bound to P1 and P5 probes labeled with biotin. The binding signals were gradually reduced by the addition of unlabeled competitive probes. Comparatively, MYB59.1 did not have DNA binding activity to P1 and P5 fragments (Supplemental Figure 6), suggesting that lack of the R2 domain may abolish the DNA binding activity of MYB59.1 (Figure 1B). These data demonstrated that MYB59.3 directly binds to the *NPF7.3* promoter, and imply that this enables regulation of *NPF7.3* transcription.

Transcription of *MYB59* and *NPF7.3* Is Responsive to External K^+ and NO_3^- Levels

Previous studies have revealed that the transcript level of *NPF7.3* is downregulated under K^+ and NO_3^--deficient conditions (Lin et al., 2008; Li et al., 2017). We asked: As the upstream regulator of *NPF7.3*, how does *MYB59* respond to external K^+ and NO_3^- levels?

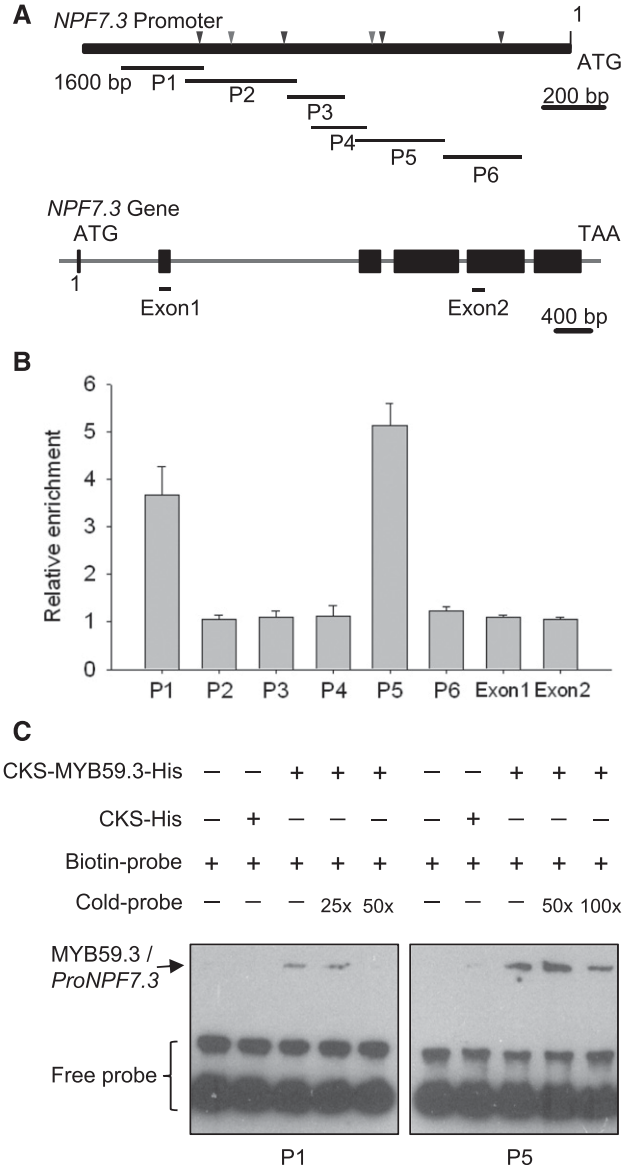

Figure 8. MYB59 Directly Binds to the *NPF7.3* Promoter.

(A) Diagram of the promoter and gene regions of *NPF7.3*. P1 to P6 together with Exon1 and Exon2 are the fragments used in ChIP-qPCR assay. Triangles with different color represent *cis*-elements. MRE and ERE are two *cis*-elements that were identified as potential MYB59-binding elements. Blue triangles represent MRE: AACCaaa, and red triangles indicate ERE: ATTTCAAA.

(B) ChIP-qPCR analysis of MYB59 DNA binding activity to the *NPF7.3* promoter. Chromatin was isolated from 10-d-old seedlings of *myb59/ProSuper:MYB59.3-FLAG* grown on K^+-sufficient medium, and immunoprecipitated with FLAG antibody. Then the six fragments were tested using qPCR. Data are shown as means ± SE ($n = 3$ independent experiments using three technical replicates).

(C) EMSA to analyze the binding activity of MYB59.3 to P1 and P5 fragments in the *NPF7.3* promoter. An excess of unlabeled probe was added to compete with labeled probe.

RT-qPCR results indicated that *MYB59* and *NPF7.3* showed similar expressions pattern in response to external nutrient (K^+ and NO_3^-) levels (Figure 9). Their expression was repressed by low K^+ and low NO_3^- treatment, but rapidly resumed when K^+ and NO_3^- were resupplied in the medium (Figure 9). This suggests that both *MYB59* and *NPF7.3* can respond to external K^+ and NO_3^- levels. These data indicated that *MYB59* functions as a positive regulator of *NPF7.3* and that both proteins operate in same pathway and adjust root-to-shoot K^+/NO_3^- transport according to external nutrient levels.

Because MYB59.3 is the functional form regulating *NPF7.3* transcription, we determined the level of MYB59.3 in response to low K^+ stress using cell-free protein degradation experiments. MYB59.3 protein was expressed in *E. coli* and then the purified protein was incubated with plant total proteins that were extracted from HK- or LK-treated wild-type plants. Our results revealed that MYB59.3 was rapidly degraded upon LK treatment (Figure 10). Moreover, addition of MG132, an inhibitor of protein degradation, totally abolished MYB59.3 degradation (Figure 10). In contrast, the level of MYB59.3 was only slightly reduced when incubated with total proteins extracted from HK-treated plants (Figure 10). These results indicated that low K^+ signaling posttranscriptionally reduces the protein level of MYB59.3 in order to downregulate *NPF7.3* transcription.

DISCUSSION

MYB59 but not *MYB48* Is Involved in the Regulation of Nutrient Transport

Arabidopsis MYB59 belongs to the R2R3-type MYB transcription factor class. A previous report showed that *MYB59* is involved in the regulation of cell cycle progression and root growth (Mu et al., 2009). In the present study, we established a function of *MYB59* in the regulation of nutrient transport. Previous studies indicated that *MYB59* and its closest homolog *MYB48* show high similarity in gene structure and amino acid sequence (Li et al., 2006). *MYB59* and *MYB48* are derived from a relatively recent duplication event,

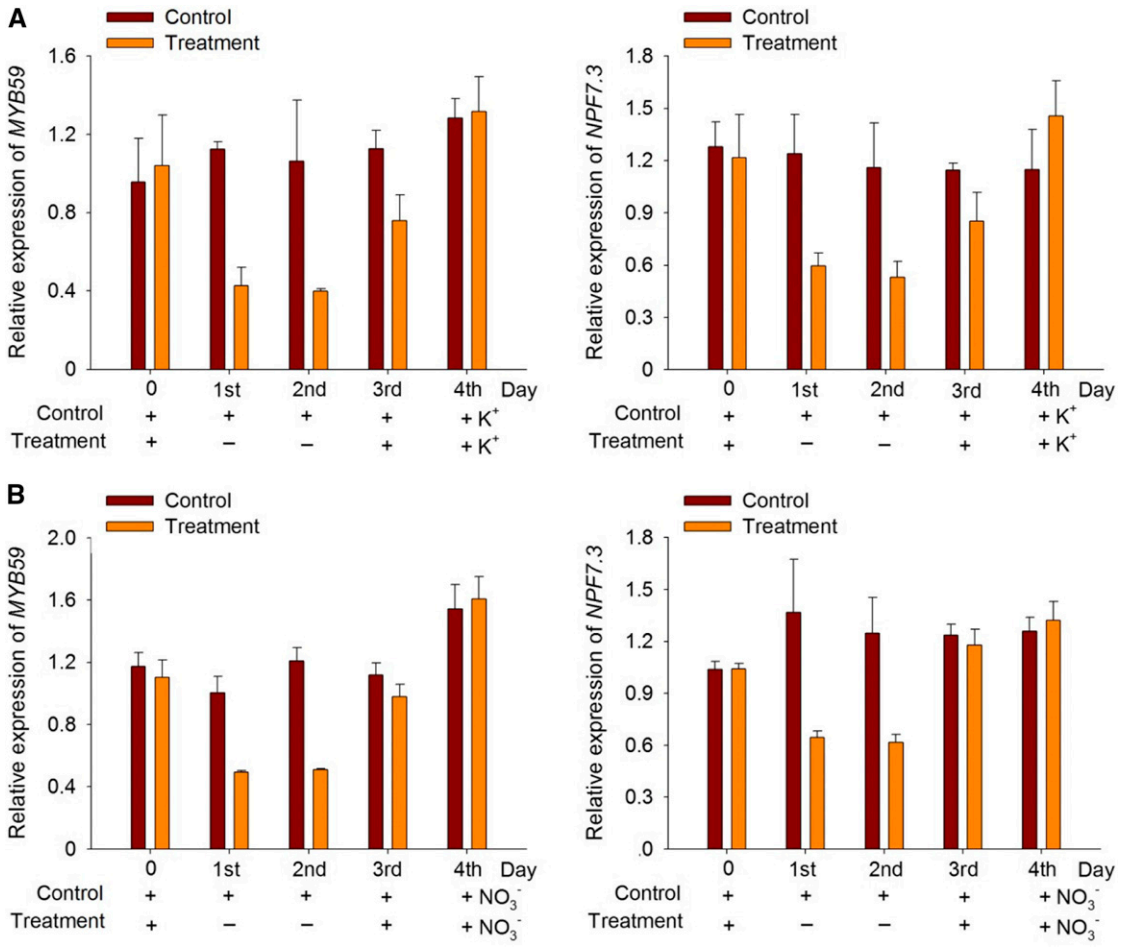

Figure 9. *MYB59* and *NPF7.3* transcription respond to external K^+/NO_3^- levels. RT-qPCR analyses of *MYB59* and *NPF7.3* expression levels after control or low K^+/NO_3^- treatment. Wild-type (Col) plants germinated on K^+/NO_3^--sufficient (5 mM) medium were transferred to K^+/NO_3^--sufficient (5 mM, $+K/+NO_3^-$) medium, or low K^+ (100 μM, -K) medium **(A)**, or low NO_3^- (0 μM, $-NO_3^-$) medium **(B)** for 2 d, respectively. Then the plants were transferred back to K^+ or NO_3^--sufficient (5 mM) medium. Roots were collected at different time points as indicated for RT-qPCR assay. RT-qPCR data are shown as means ±SE ($n = 3$ independent experiments as described in Methods

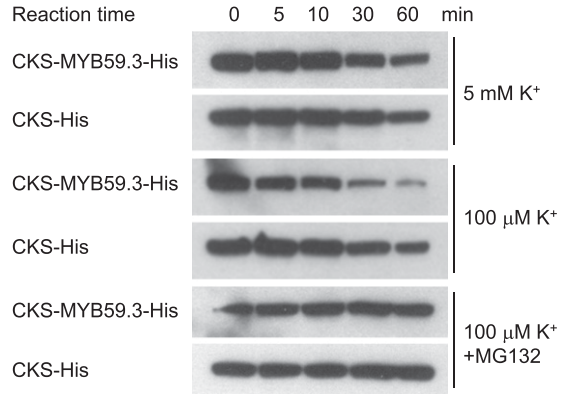

Figure 10. MYB59.3 protein is degraded after low K^+ stress. Cell-free degradation assay for MYB59.3. MYB59.3 protein (CKS-MYB59.3-His) was expressed in *E. coli*. Then, the purified protein was incubated with plant total proteins that were extracted from HK (5 mM)- or LK (100 μM)- treated wild-type plants. The proteasome inhibitor MG132 (10 μM) was added to reduce the degradation of ubiquitin-conjugated proteins. The abundance of MYB59.3 protein was determined by immunoblotting with an anti-His antibody. Recombinant CKS-His was used as control.

and they share 74.2% nucleotide sequence identity in their coding regions (Chen et al., 2006; Li et al., 2006). In addition, both of them play roles in the jasmonic acid signaling network (Hickman et al., 2017), suggesting their functional redundancy. To test whether *MYB59* and *MYB48* were redundant in the regulation of K^+/NO_3^- transport, the phenotypes of their single and double mutants were tested. With the use of the CRISPR/CRISPR-associated protein (Cas) 9 technique, four independent mutant lines of *MYB48* were obtained. However, none of them displayed a low K^+ sensitive phenotype like the *myb59* mutant (Supplemental Figure 7A). In addition, three *myb59 myb48* double mutant lines were also constructed using CRISPR/Cas9 in the *myb59* background. The double mutant plants showed similar phenotype as the *myb59* single mutants (Supplemental Figure 7B). These analyses indicated that only *MYB59* rather than *MYB48* is involved in Arabidopsis response to low K^+ stress.

MYB59 and *MYB48* Genes Undergo Alternative Splicing

Previous reports revealed that both *MYB59* and *MYB48* undergo similar alternative splicing and have four distinctively spliced transcripts (Li et al., 2006). In the present study, we report that expression of the longest transcript (*MYB59.3*) is sufficient to bring about the K^+-related function of MYB59 in Arabidopsis (Figure 2B). Moreover, a recent study reported that both *Arabidopsis MYB59* and *MYB48* showed alternative splicing only in the response to K^+ deficiency, but not to other nutrient-deficient conditions (Nishida et al., 2017). After low K^+ treatment, the total transcript levels of *MYB59* and *MYB48* were reduced, but their longest transcripts *MYB59.3* and *MYB48.3* were significantly increased (Nishida et al., 2017).

We also observed alternative splicing of *MYB59*. Low K^+ treatment repressed the total transcript amount of *MYB59* (Figure 9), but resulted in enhanced accumulation of the *MYB59.3* transcript (Supplemental Figure 8). Resupply of K^+ rapidly restored the normal expression pattern of all three spliced transcripts (Supplemental Figure 8). In contrast, *NPF7.3* forms only one transcript that was downregulated after low K^+ treatment (Figure 9). The total transcript amount of *MYB59* perfectly matched the expression change of *NPF7.3* in Arabidopsis response to external K^+ levels (Figure 9). But there is a discrepancy between *MYB59.3* and *NPF7.3* in the accumulation of their transcript levels after low K^+ treatment. According to the results from our phenotype and genetic analyses, *MYB59.3* is a positive regulator of *NPF7.3* and promotes *NPF7.3* expression (Figure 2B; Supplemental Figure 2). Therefore, the increased *MYB59.3* transcript levels are unlikely to be the reason for *NPF7.3* repression under low K^+ conditions. We hypothesized that low K^+ signaling may posttranscriptionally reduce the protein level or transcriptional activity of MYB59.3, which downregulates the *NPF7.3* transcription. MYB59.3 proteins may be degraded, phosphorylated, or modified under K^+-deficient conditions. Such regulation represents a common mechanism for a rapid on-and-off switch of MYB transcription factor activity (Pireyre and Burow, 2015). Indeed, we observed that MYB59.3 protein was degraded after low K^+ stress (Figure 10), resulting in the downregulation of *NPF7.3* transcription. In this regard, the induction of *MYB59.3* transcription after low K^+ stress may be a result of a feedback response.

Transcriptional Regulation of Transporter Proteins Is Important for K^+ Homeostasis in Plants

Transcriptional regulation provides an essential strategy in plant response to K^+ deficiency. For example, the transcript levels of K^+ transporter genes are upregulated under K^+-deficient conditions in order to enhance high-affinity K^+ uptake in plant roots (Wang and Wu, 2013, 2017). At the same time, the root-to-shoot K^+ transport must be reduced to keep sufficient K^+ in roots, and this represents an important adaptive mechanism to maintain root activity and the K^+ balance between root and shoot. Upon K^+ depletion in the soil, it is mandatory for the root to sustain a minimal concentration of K^+ in order to maintain the required membrane potential and osmotic balance. In contrast, if sufficient K^+ were available for growth of the plants, the stem and young leaves represent a major sink that requires large amount of K^+. Under this condition, more K^+ will be transported toward shoots to support plant growth. Therefore, root-to-shoot K^+ transport needs to be fine-tuned according to external K^+ levels.

In the present study, we show that the modulation of root-to-shoot K^+ translocation was controlled by *NPF7.3* via transcriptional regulation. Furthermore, *NPF7.3* transcription was regulated by MYB59, and *MYB59* transcription was also modulated by some unknown components in this process. Our data indicate that both *MYB59* and *NPF7.3* can respond to external K^+ levels (Figure 9). Plants accurately control the transcript levels of *MYB59* and *NPF7.3* to achieve the proper K^+ distribution between roots and shoots. Under K^+-deficient conditions, plants need to represses *MYB59* and *NPF7.3* expression to keep enough K^+ in roots and maintain proper root activity. However, downregulation of *MYB59* and *NPF7.3* expression under low K^+ conditions does not mean plants do not need them. In loss-of-function mutants of *MYB59* or *NPF7.3*, root-to-shoot K^+ transport (Figure 6C) was largely abolished, causing K^+-deficient symptoms to appear in

mutant shoots much earlier than in wild-type plants (Figure 5A). Therefore, the transcript levels of *Arabidopsis MYB59* and *NPF7.3* need to be accurately fine-tuned in response to external K^+ levels. In addition, we noticed that *MYB59* expression was upregulated in *npf7.3* mutant plants (Figure 6D), suggesting that there is feedback regulation of *MYB59* transcription when *NPF7.3* function is disrupted.

MYB59 and *NPF7.3* Form a Regulatory Module for Coordination of K^+/NO_3^- Transport

Sufficient supplies of potassium and nitrogen are critical for crop yield and quality. However, current fertilization practices in some agricultural regions (e.g., in East Asia) limit the development of agriculture and result in many problems. For example, overuse of nitrogen fertilizer in conjunction with a lack of potash fertilizer in China not only significantly reduces nitrogen utilization efficiency, but also causes air/water/soil pollution and ecosystem deterioration (Pettigrew, 2008; Guo et al., 2010; Zhang, 2017). The molecular mechanism underlying this phenomenon is the coordination of K/N utilization. Previous studies found that the dual-role transporter NPF7.3 plays essential roles in K^+/NO_3^- co-transport in Arabidopsis (Lin et al., 2008; Li et al., 2017). A low K^+ supply could reduce NO_3^- transport in *npf7.3* mutants (Figures 5D and 5F), and conversely a low NO_3^- supply also reduces K^+ transport toward shoot in *npf7.3* mutant (Li et al., 2017). The transcript level of *NPF7.3* is responsive to external K and N levels (Lin et al., 2008; Li et al., 2017), suggesting that *NPF7.3* is part of an important mechanism for maintaining K/N balance. In the present study, we identified a transcription factor that positively regulates *NPF7.3* expression to balance K^+/NO_3^- transport (Figure 11). Under K^+/NO_3^--sufficient conditions, MYB59 binds to the *NPF7.3* promoter and facilitates NPF7.3-mediated root-to-shoot K^+/NO_3^- transport. When plants are subjected to K^+/NO_3^--deficient stresses, *MYB59* is downregulated, which subsequently impairs the accumulation of the *NPF7.3* transcript. Therefore, root-to-shoot K^+/NO_3^- transport is restricted in order to balance the K^+/NO_3^- distribution between root and shoot. In conclusion, the present study establishes a central role for transcriptional regulation as a mechanism of K^+/NO_3^- coordination in plants response to fluctuating nutrient environments.

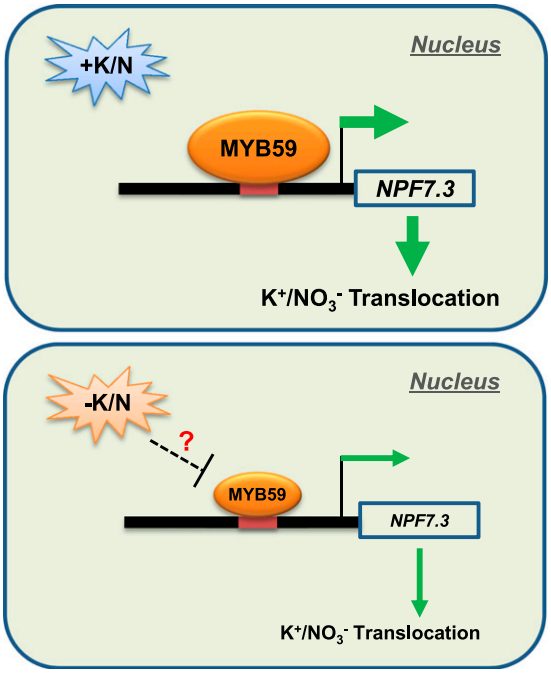

Figure 11. Working model of *NPF7.3* transcriptional regulation by MYB59 in Arabidopsis response to low K^+/NO_3^- stresses. Under K^+/NO_3^--sufficient conditions, MYB59 directly binds to the *NPF7.3* promoter and facilitates NPF7.3-mediated root-to-shoot K^+/NO_3^- transport. When plants are subjected to K^+/NO_3^--deficient stresses, *MYB59* is downregulated and subsequently inhibits the transcript level of *NPF7.3*. Therefore, root-to-shoot K^+/NO_3^- transport is restricted.

METHODS

Plant Materials

The Arabidopsis (*Arabidopsis thaliana*) transfer DNA insertion lines (Columbia ecotype, Col-0), including *myb59-1* (GABI_627C09), *npf7.3* (SALK_043036), and *hak5* (SALK_005604), were obtained from Nottingham Arabidopsis Stock Centre or Arabidopsis Biological Resource Center. The *lks2* and *skor* mutants were obtained as described previously (Li et al., 2017).

To produce the CRISPR/Cas9 construct, the vector pCBC-DT1T2 (Xing et al., 2014) was used as the template and a DT1-BsF/DT1-F0/DT2-R0/DT2-BsR four-primer mixture (as mentioned in Supplemental Table 2) was used with DT1-F0/DT2-R0 diluted 20-fold with DT1-BsF or DT2-BsR, resulting in DT1T2-PCR. To clone the DT1T2-PCR product into the pHSE401 vector (Xing et al., 2014), the restriction/ligation reaction was performed in a total volume of 15 μL, which contained 2 μL DT1T2-PCR product, 2 μL pHSE401 vector, 1.5 μL 10× T4 Buffer (New England Biolabs, NEB), 1.5 μL 10× BSA, 1 μL *Bsa*I (NEB), 1 μL T4 Ligase (NEB), 6 μL distilled deionizedwater. The reaction was performed at 37°C for 5 h, 50°C for 5 min, and 80°C for 10 min, resulting the final CRISPR/Cas9 construct. To generate the *myb59-2* mutant, the CRISPR/Cas9 construct for *MYB59* was transformed into wild-type (Col-0) plants. The CRISPR/Cas9 construct for *MYB48* was transformed into wild-type (Col-0) plants or the *myb59-1* mutant, respectively, generating *myb48* mutants and *myb59 myb48* double mutants. Genomic DNA from plants in the T_1 generation was sequenced for construct verification.

The *MYB59* genomic sequence was cloned into the pCAMBIA1300 vector (Cambia) driven by its native promoter, and this construct was transformed into the *myb59-1* mutant to obtain two complementation lines (COM1 and COM2). Sequences encoding each of the three *MYB59* transcripts driven by the native promoter were cloned separately into the pCAMBIA1305 vector (Cambia) and then transformed into the *myb59-1* mutant to obtain complementation lines corresponding to each transcript (*MYB59.1* COM, *MYB59.2* COM, *MYB59.3* COM). The *NPF7.3* genomic sequence was cloned into the pCAMBIA1300 vector driven by *PHO1* promoter, and was transformed into *myb59-1* mutant and *npf7.3* mutant, respectively, to generate *myb59-1/ProPHO1:NPF7.3* and *npf7.3/ProPHO1:NPF7.3* plants. *MYB59* and *NPF7.3* promoter fragments were cloned into the pCAMBIA1381 vector (Cambia) and were transformed into wild-type plants to generate *ProMYB59:GUS* or *ProNPF7.3:GUS* plants, respectively. The *myb59-1/ProSuper:MYB59.3-FLAG* lines were generated by cloning the coding sequence of *MYB59.3* into the SUPER1300 vector (Cambia) and transforming into *myb59-1* mutant. Homozygous T_4 transgenic plants were used.

Phenotypic Analyses and Growth Conditions

The K^+-sufficient medium and low-K^+ medium for phenotypic analyses were modified from MS medium as follows: 1.5 mM $MgSO_4$ was unchanged, 1.25 mM KH_2PO_4 and 2.99 mM $CaCl_2$ were replaced by 1.25 mM $NH_4H_2PO_4$ and 2.99 mM $Ca(NO_3)_2$, and 20.6 mM NH_4NO_3 and 18.79 mM KNO_3 were removed. The actual and final K^+ concentration in the K^+-sufficient medium and low-K^+ medium were adjusted to 5 mM and 100 μM, respectively, by adding KCl. For the phenotypic analyses using different concentrations of K^+, media were also supplemented with KCl.

For NO_3^- treatments, media were modified from K^+-sufficient medium as follows: 1.5 mM $MgSO_4$ and 1.25 mM $NH_4H_2PO_4$ were unchanged, 2.99 mM $Ca(NO_3)_2$ was replaced by 2.99 mM $CaCl_2$, and then either 5 mM KNO_3 or 5 mM KCl was added, respectively, representing NO_3^--sufficient medium or NO_3^--deficient medium.

All the media used in the study contained 0.9% (w/v) agar and 3% (w/v) Suc. Seeds were surface sterilized using 6% (v/v) NaClO and germinated on K^+-sufficient medium or low-K^+ medium at 22°C under constant illumination (60 μmol m^{-2} s^{-1}) for 10 d. For phenotypic assays, four plates were considered four biological replicates in one independent experiment. Each plate contained 7–10 seedlings for each plant material. In one phenotype test, at least three independent experiments were performed. A photograph of one plate is shown in a figure to represent one phenotypic test.

For seed harvest, Arabidopsis plants were grown in a potting soil mixture (rich soil/vermiculite = 2:1, v/v) and kept in a growth chamber (22°C, illumination at 120 μmol m^{-2} s^{-1} for a 16 h daily light period; the relative humidity was ~70%).

Measurement of K^+ and NO_3^- Content in Plant Tissues

Seedlings were germinated and grown on K^+-sufficient medium or low K^+ medium for 10 d, and then shoots and roots were harvested separately. The plant samples were washed thoroughly three times with double-distilled water.

For K^+ content analyses, samples were dried at 80°C for 24 h to a constant weight and the dry weight was measured. Samples were treated in a muffle furnace at 300°C for 1 h and at 575°C for 5 h and dissolved in 0.1 N HCl. The K^+ concentrations were measured using the 4100-MP Atomic Emission Spectrometrysystem (Agilent). Three biological replicates were used in one independent experiment. For low K^+ treatment, ~90-100 individual seedlings from two plates were collected and used as one biological replicate. For K^+-sufficient treatment, ~40–45 individual seedlings from one plate were collected and used as one biological replicate. Three independent experiments were performed in one measurement analysis.

For NO_3^- content analyses, the fresh weight of plant shoots and roots was measured. Plant tissues were boiled in double-distilled water for 20 min and then frozen at −80°C. The NO_3^- concentrations of plant samples were measured using HPLC. Three biological replicates were used in one independent experiment. For low K^+ treatment, ~80–100 individual seedlings from two plates were collected and used as one biological replicate. For K^+-sufficient treatment, ~20–25 individual seedlings from one plate were collected and used as one biological replicate. Three independent experiments were performed in one measurement analysis.

Measurement of K^+ and NO_3^- Content in Xylem Sap

Arabidopsis seeds were germinated on K^+-sufficient medium for 10 d and then transferred into vermiculite. Plants were irrigated with 1/4-strength nutrient solution containing 5 mM K^+ (K^+ sufficient) or 100 μM K^+ (K^+ deficient). The nutrient solution was renewed every week. After growing in a growth chamber for 20 d, the plant shoots were excised and xylem sap was collected using capillaries within 2 h. Three biological replicates were used in one independent experiment. For each replicate, the xylem sap was collected from 20–24 individual plants. The total volume for each replicate was ~40-60 μL. The K^+ and NO_3^- concentrations in xylem sap were measured using the 4100-MP Atomic Emission Spectrometry system or HPLC.

Transcription Analyses

For both RT-PCR and RT-qPCR analyses, total RNA was extracted from roots of 8-d-old seedlings by using the TriZOL reagent (Invitrogen), and then treated with DNase I (RNase Free, Takara) to eliminate genomic DNA contamination. The complementary DNA (cDNA) was synthesized by SuperScript^{II} RNase reverse transcriptase (Invitrogen). Oligo (dT) primers (Promega) and Random Hexamer primers (Promega) were used for RT-PCR and RT-qPCR analyses, respectively.

For RT-PCR, ~80–100 individual seedlings from two plates were collected and used as one sample. Three independent experiments were performed. The *Elongation Factor 1α* gene was used as an internal standard for normalization of gene expression levels. Two pairs of specifically designed primers were used to amplify *MYB59* transcripts of different sizes: MYB59_fw2 and MYB59_rev2 as described (Li et al., 2006), MYB59_fw3 and MYB59_rev3 (see Supplemental 2 for all primer sequences). The primers MYB59_fw2 and MYB59_rev2 were used to amplify *MYB59.1* (expected size 643 bp). PCR was performed for 30 cycles, each at 94°C for 30 s, 57°C for 30 s, and 72°C for 45 s. The primers MYB59_fw3 and MYB59_rev3 were used to amplify *MYB59.2* (expected size 336 bp) and *MYB59.3* (expected size 304 bp). PCR was performed for 35 cycles, each with 94°C for 30 s, 50°C for 30 s, and 72°C for 30 s.

RT-qPCR was conducted using a Power SYBR Green PCR Master Mix (Applied Biosystems, USA) on a 7500 Real Time PCR System machine (Applied Biosystems). The amplification reactions were performed in a total volume of 20 μL, which contained 10 μL SYBR Green premix, 7 μL distilled, deionized water, 2 μL forward and reverse primers (1 μM), and 1 μL cDNA. PCR was conducted as follows: 95°C for 10 min, followed by 40 cycles of 95°C for 15 s and 60°C for 1 min. For NO_3^- treatment experiments, Eukaryotic translation Initiation Factor 4A-1 was used as an internal standard for normalization of gene expression levels. For other experiments, RT-qPCR results were calculated by normalization to *Actin2/8*. Three biological replicates were used in one independent RT-qPCR experiment. Each replicate contained 80–100 individual seedlings from two plates. Three independent experiments were performed in one RT-qPCR analysis.

Transcriptional Activation Assays in Yeast

cDNAs encoding three of the *MYB59* transcripts were separately cloned into the pGBKT7/BD vector (Clontech) containing the GAL4 DNA binding domain. Either pBD-MYB59.1, pBD-MYB59.2, pBD-MYB59.3, the positive control pBD-GAL4, or the negative control pBD vector was transformed into the yeast strain AH109 (Clontech). The transformed strains were cultured on synthetic dropout nutrient medium without tryptophan (SD/-TRP) plates and confirmed by PCR, and then were spotted on SD/-TRP or SD/-TRP-HIS (histidine) plates by diluting to different concentrations. Medium lacking Trp (SD/-TRP) was used to indicate the presence of constructs in the pGBKT7/BD vector, and medium without both Trp and His (SD/-TRP-HIS) was to identify whether these clones could activate the expression of the reporter gene *HIS3* (Reece-Hoyes and Marian Walhout, 2012). The transcription activation activity of each transcript was evaluated according to the growth status of the corresponding yeast cells. The LacZ marker gene was examined by X-gal assay.

ChIP-qPCR Assays

Seedlings of *myb59-1/ProSuper:MYB59.3-FLAG* were germinated on K^+-sufficient medium for 10 d, and then roots from 2000–2500 individual seedlings (about 0.5–1 g fresh weight) were collected as one replicate for

ChIP experiments. The samples were first crosslinked using formaldehyde. Then the crosslinked nuclei were purified and sonicated to shear the chromatin into suitably sized fragments. The anti-FLAG antibody (MBL, Lot number: M185-3L) was used to immunoprecipitate protein/DNA complexes from the chromatin. Anti-FLAG antibody (5-10 μL) was added to positive sample of 2 mL. The DNA in the complexes was recovered and analyzed by qPCR methods. qPCR was performed for 40 cycles, each at 95°C for 15 s, 50°C for 20 s, and 60°C for 45 s. Six primer combinations were used to amplify fragments within the promoter of *NPF7.3*. Two exon fragments in the *NPF7.3* coding sequence were amplified as internal controls. The relative enrichment of each fragment was calculated by comparing samples treated with antibodies to samples treated without antibodies. Three technical replicates were used in one independent experiment. Three independent experiments were performed.

EMSA

EMSA assays were performed using the LightShift Chemiluminescent EMSA kit (Pierce) following the manufacturer's protocol. The recombinant proteins CKS-MYB59.3-His, CKS-MYB59.1-His and CKS-His were expressed in and purified from *E. coli*. Two fragments (P1 and P5) in the *NPF7.3* promoter were obtained by PCR, and either left unlabeled or labeled with 5′-biotin. The unlabeled fragments of the same sequences were used as competitors, and the CKS-His protein alone was used as the negative control.

Cell-Free Degradation Assays

Five-d-old wild-type seedlings were transferred to K^+-sufficient medium (5 mM K^+), low-K^+ medium (100 μM K^+), or low-K^+ medium containing 10 μM MG132 for 3 d. Roots of 200–250 individual seedlings from two plates were collected and used as one replicate. The roots were harvested and ground into a fine powder in liquid nitrogen. Total proteins were extracted in degradation buffer containing 25 mM Tris-HCl, pH7.5; 10 mM $MgCl_2$; 10 mM NaCl; 4 mM phenylmethylsulfonyl fluoride; 5 mM dithiothreitol; and 10 mM ATP. The protein concentration was determined using the Bio-Rad protein assay. To monitor the degradation of recombinant protein CKS-MYB59.3-His, 250 ng purified recombinant protein was incubated in 20 μL of root protein extract (50 μg) at 22°C for the indicated time periods. Recombinant CKS-His was used as a control. The abundance of CKS-MYB59.3-His or CKS-His was analyzed by immunoblotting with an anti-His antibody (EASYBIO, Lot number: BE2019) used at a 1:5000 dilution.

$^{86}Rb^+$ Uptake Assay

$^{86}Rb^+$ uptake assays were performed as described previously (Zhao et al., 2016). Seven-d-old seedlings that were grown on MS medium were transferred to LK medium for 2 d. Then, the plants were incubated in 1.5 mL uptake solution (5 mM MES and 0.2 mM $CaCl_2$) that was K^+ free and supplemented with 100 μM RbCl containing 0.005 μCi/nmol $^{86}Rb^+$ (Amersham Biosciences). At the end of the uptake period, plants were blotted with tissue paper and immediately washed two times for 30 min in 4°C washing solution (K^+ free and supplemented with 1.75 mM nonradio-labeled RbCl). The radioactivity in plants was measured with a scintillation counter (Perkin-Elmer 1450 MicroBeta TriLux) after the addition of 1 mL scintillation liquid. Three biological replicates were used in one independent experiment. The fresh weight of 12 individual seedlings was measured as one replicate before the materials were used for $^{86}Rb^+$ uptake assays.

RNA Isolation and RNA-seq

Five-d-old seedlings were transferred from MS medium to low K^+ medium for 2 d. Total RNA was extracted from roots using the TriZOL reagent (Invitrogen). RNA degradation was monitored on 1% agarose gels, and RNA purity was checked using the NanoPhotometer® spectrophotometer (IMPLEN). RNA integrity was assessed using the RNA Nano 6000 Assay Kit of the Agilent Bioanalyzer 2100 system (Agilent Technologies). Sequencing libraries were generated using the NEBNext® Ultra TM RNA Library Prep Kit for Illumina® (NEB). The library preparations were sequenced on an Illumina Hiseq 4000 platform, and 150-bp paired-end reads were generated. Raw sequence data were cleaned by filtering out reads containing unknown bases (more than 10% of the total bases), adapter sequences, or more than 50% of the total bases with quality values of <5.

Accession Numbers

Sequence data for the genes described in this article can be found in The Arabidopsis Information Resource database (https://www.arabidopsis.org) under the following accession numbers: At5g59780 for *MYB59*, At3g46130 for *MYB48*, At3g23430 for *PHO1*, At1g32450 for *NPF7.3*, At4g13420 for *HAK5*, At3g02850 for *SKOR*. Germplasm used included *myb59-1* (GABI_627C09), *npf7.3* (SALK_043036), *hak5* (SALK_005604), along with the *lks2* and *skor* mutants (Li et al., 2017).

Supplemental Data

Supplemental Figure 1. Dry weight of various plant materials.

Supplemental Figure 2. Phenotype of the *MYB59.3* overexpressing line.

Supplemental Figure 3. Phenotype of the *hak5* mutant and $^{86}Rb^+$ uptake test in *myb59* and *npf7.3* mutants.

Supplemental Figure 4. Phenotype of the *skor* mutant.

Supplemental Figure 5. Phenotypes of the transgenic lines expressing *NPF7.3* driven by the *PHO1* promoter.

Supplemental Figure 6. EMSA analysis of the binding activity of MYB59.1 to the *NPF7.3* promoter.

Supplemental Figure 7. Phenotypes of the *myb48* single mutant and the *myb59 myb48* double mutant.

Supplemental Figure 8. RT-PCR analysis showing the changes of three *MYB59* transcripts in the Arabidopsis response to low K^+ stress.

Supplemental Table 1. Expression analyses of K^+-related genes in the *myb59* mutant using RNA-seq method.

Supplemental Table 2. Primer sequences used in this study.

ACKNOWLEDGMENTS

We thank Dr. Qijun Chen for providing the CRISPR/Cas9 vector. We thank Dr. Yan Guo for providing the pCAMBIA1305-FLAG and pTrc-CKS vectors. We also thank Dr. Reinhard Kunze (Free University Berlin, Germany) for help on this article. This work was supported by grants from the National Natural Science Foundation of China (NSFC) (31570243, 31622008, and 31761133011 to Y.W.) and the Deutsche Forschungsgemeinschaft (DFG) (Ku 931/18-1 to J.K.).

AUTHOR CONTRIBUTIONS

J.L., W.-H.W., J.K., and Y.W. designed the research; X.-Q.D., F.-L.W., H.L., S.J., and M.Y. conducted the experiments; X.-Q.D. and Y.W. wrote and revised the article.

Received September 5, 2018; revised November 29, 2018; accepted February 8, 2019; published February 13, 2019.

REFERENCES

Adams, E., and Shin, R. (2014). Transport, signaling, and homeostasis of potassium and sodium in plants. J. Integr. Plant Biol. **56:** 231–249.

Agarwal, M., Hao, Y., Kapoor, A., Dong, C.H., Fujii, H., Zheng, X., and Zhu, J.K. (2006). A R2R3 type MYB transcription factor is involved in the cold regulation of CBF genes and in acquired freezing tolerance. J. Biol. Chem. **281:** 37636–37645.

Baumann, K., Perez-Rodriguez, M., Bradley, D., Venail, J., Bailey, P., Jin, H., Koes, R., Roberts, K., and Martin, C. (2007). Control of cell and petal morphogenesis by R2R3 MYB transcription factors. Development **134:** 1691–1701.

Blevins, D.G., Barnett, N.M., and Frost, W.B. (1978). Role of potassium and malate in nitrate uptake and translocation by wheat seedlings. Plant Physiol. **62:** 784–788.

Chen, Y.H., et al. (2006) The MYB transcription factor superfamily of Arabidopsis: Expression analysis and phylogenetic comparison with the rice MYB family. Plant Mol. Biol. **60:** 107–124.

Chen, Y.F., Wang, Y., and Wu, W.H. (2008). Membrane transporters for nitrogen, phosphate and potassium uptake in plants. J. Integr. Plant Biol. **50:** 835–848.

Clarkson, D.T., and Hanson, J.B. (1980). The mineral nutrition of higher plants. Annu. Rev. Plant Biol. **31:** 239–298.

Drechsler, N., Zheng, Y., Bohner, A., Nobmann, B., von Wirén, N., Kunze, R., and Rausch, C. (2015). Nitrate-dependent control of shoot K homeostasis by the nitrate transporter1/peptide transporter family member NPF7.3/NRT1.5 and the stelar K^+ outward rectifier SKOR in *Arabidopsis.* Plant Physiol. **169:** 2832–2847.

Dubos, C., Stracke, R., Grotewold, E., Weisshaar, B., Martin, C., and Lepiniec, L. (2010). MYB transcription factors in *Arabidopsis.* Trends Plant Sci. **15:** 573–581.

Feller, A., Machemer, K., Braun, E.L., and Grotewold, E. (2011). Evolutionary and comparative analysis of MYB and bHLH plant transcription factors. Plant J. **66:** 94–116.

Gaymard, F., Pilot, G., Lacombe, B., Bouchez, D., Bruneau, D., Boucherez, J., Michaux-Ferrière, N., Thibaud, J.B., and Sentenac, H. (1998). Identification and disruption of a plant shaker-like outward channel involved in K^+ release into the xylem sap. Cell **94:** 647–655.

Gierth, M., Mäser, P., and Schroeder, J.I. (2005). The potassium transporter *AtHAK5* functions in K^+ deprivation-induced high-affinity K^+ uptake and *AKT1* K^+ channel contribution to K^+ uptake kinetics in Arabidopsis roots. Plant Physiol. **137:** 1105–1114.

Guo, J.H., Liu, X.J., Zhang, Y., Shen, J.L., Han, W.X., Zhang, W.F., Christie, P., Goulding, K.W.T., Vitousek, P.M., and Zhang, F.S. (2010). Significant acidification in major Chinese croplands. Science **327:** 1008–1010.

Hamburger, D., Rezzonico, E., MacDonald-Comber Petétot, J., Somerville, C., and Poirier, Y. (2002). Identification and characterization of the Arabidopsis *PHO1* gene involved in phosphate loading to the xylem. Plant Cell **14:** 889–902.

Han, M., Wu, W., Wu, W.H., and Wang, Y. (2016). Potassium transporter KUP7 is involved in K^+ acquisition and translocation in *Arabidopsis* root under K^+-limited conditions. Mol. Plant **9:** 437–446.

Hickman, R., et al. (2017). Architecture and dynamics of the jasmonic acid gene regulatory network. Plant Cell **29:** 2086–2105.

Hirsch, R.E., Lewis, B.D., Spalding, E.P., and Sussman, M.R. (1998). A role for the AKT1 potassium channel in plant nutrition. Science **280:** 918–921.

Jung, C., Seo, J.S., Han, S.W., Koo, Y.J., Kim, C.H., Song, S.I., Nahm, B.H., Choi, Y.D., and Cheong, J.J. (2008). Overexpression of *AtMYB44* enhances stomatal closure to confer abiotic stress tolerance in transgenic Arabidopsis. Plant Physiol. **146:** 623–635.

Kim, M.J., Ruzicka, D., Shin, R., and Schachtman, D.P. (2012). The Arabidopsis AP2/ERF transcription factor RAP2.11 modulates plant response to low-potassium conditions. Mol. Plant **5:** 1042–1057.

Leigh, R.A., and Wyn Jones, R.G. (1984). A hypothesis relating critical potassium concentrations for growth to the distribution and functions of this ion in the plant cell. New Phytol. **97:** 1–13.

Léran, S., et al. (2014). A unified nomenclature of NITRATE TRANSPORTER 1/PEPTIDE TRANSPORTER family members in plants. Trends Plant Sci. **19:** 5–9.

Li, H., Yu, M., Du, X.Q., Wang, Z.F., Wu, W.H., Quintero, F.J., Jin, X.H., Li, H.D., and Wang, Y. (2017). NRT1.5/NPF7.3 functions as a proton-coupled H^+/K^+ antiporter for K^+ loading into the xylem in Arabidopsis. Plant Cell **29:** 2016–2026.

Li, J., Li, X., Guo, L., Lu, F., Feng, X., He, K., Wei, L., Chen, Z., Qu, L.J., and Gu, H. (2006). A subgroup of *MYB* transcription factor genes undergoes highly conserved alternative splicing in *Arabidopsis* and rice. J. Exp. Bot. **57:** 1263–1273.

Li, L., Yu, X., Thompson, A., Guo, M., Yoshida, S., Asami, T., Chory, J., and Yin, Y. (2009). Arabidopsis MYB30 is a direct target of BES1 and cooperates with BES1 to regulate brassinosteroid-induced gene expression. Plant J. **58:** 275–286.

Lin, S.H., Kuo, H.F., Canivenc, G., Lin, C.S., Lepetit, M., Hsu, P.K., Tillard, P., Lin, H.L., Wang, Y.Y., Tsai, C.B., Gojon, A., and Tsay, Y.F. (2008). Mutation of the Arabidopsis NRT1.5 nitrate transporter causes defective root-to-shoot nitrate transport. Plant Cell **20:** 2514–2528.

Meng, S., Peng, J.S., He, Y.N., Zhang, G.B., Yi, H.Y., Fu, Y.L., and Gong, J.M. (2016). *Arabidopsis* NRT1.5 mediates the suppression of nitrate starvation-induced leaf senescence by modulating foliar potassium level. Mol. Plant **9:** 461–470.

Mengel, K., and Kirkby, E.A. (2001). Principles of plant nutrition, (Dordrecht, The Netherlands: Kluwer Academic Publishers).

Mu, R.L., et al. (2009). An R2R3-type transcription factor gene *AtMYB59* regulates root growth and cell cycle progression in *Arabidopsis.* Cell Res. **19:** 1291–1304.

Nishida, S., Kakei, Y., Shimada, Y., and Fujiwara, T. (2017). Genome-wide analysis of specific alterations in transcript structure and accumulation caused by nutrient deficiencies in *Arabidopsis thaliana.* Plant J. **91:** 741–753.

O'Brien, J.A., Vega, A., Bouguyon, E., Krouk, G., Gojon, A., Coruzzi, G., and Gutiérrez, R.A. (2016). Nitrate transport, sensing, and responses in plants. Mol. Plant **9:** 837–856.

Peng, J. (2009). Gibberellin and jasmonate crosstalk during stamen development. J. Integr. Plant Biol. **51:** 1064–1070.

Pettigrew, W.T. (2008). Potassium influences on yield and quality production for maize, wheat, soybean and cotton. Physiol. Plant. **133:** 670–681.

Pireyre, M., and Burow, M. (2015). Regulation of MYB and bHLH transcription factors: A glance at the protein level. Mol. Plant **8:** 378–388.

Prouse, M.B., and Campbell, M.M. (2012). The interaction between MYB proteins and their target DNA binding sites. Biochim. Biophys. Acta **1819:** 67–77.

Pyo, Y.J., Gierth, M., Schroeder, J.I., and Cho, M.H. (2010). High-affinity K^+ transport in Arabidopsis: AtHAK5 and AKT1 are vital for seedling establishment and postgermination growth under low-potassium conditions. Plant Physiol. **153:** 863–875.

Reece-Hoyes, J.S., and Marian Walhout, A.J. (2012). Yeast one-hybrid assays: A historical and technical perspective. Methods **57:** 441–447.

Rubio, F., Santa-María, G.E., and Rodríguez-Navarro, A. (2000). Cloning of Arabidopsis and barley cDNAs encoding HAK potassium transporters in root and shoot cells. Physiol. Plant. **109:** 34–43.

Triplett, E.W., Barnett, N.M., and Blevins, D.G. (1980). Organic acids and ionic balance in xylem exudate of wheat during nitrate or sulfate absorption. Plant Physiol. **65:** 610–613.

Wang, Y., and Wu, W.H. (2013). Potassium transport and signaling in higher plants. Annu. Rev. Plant Biol. **64:** 451–476.

Wang, Y., and Wu, W.H. (2017). Regulation of potassium transport and signaling in plants. Curr. Opin. Plant Biol. **39:** 123–128.

Wang, R., Tischner, R., Gutiérrez, R.A., Hoffman, M., Xing, X., Chen, M., Coruzzi, G., and Crawford, N.M. (2004). Genomic analysis of the nitrate response using a nitrate reductase-null mutant of *Arabidopsis.* Plant Physiol. **136:** 2512–2522.

Wang, X., Niu, Q.W., Teng, C., Li, C., Mu, J., Chua, N.H., and Zuo, J. (2009). Overexpression of *PGA37/MYB118* and *MYB115* promotes vegetative-to-embryonic transition in *Arabidopsis.* Cell Res. **19:** 224–235.

Wang, Y.Y., Hsu, P.K., and Tsay, Y.F. (2012). Uptake, allocation and signaling of nitrate. Trends Plant Sci. **17:** 458–467.

White, P.J. (2012). Long-distance transport in the xylem and phloem. *In*: Marschner's Mineral Nutrition of Higher Plants, P. Marschner, ed (Amsterdam: Elsevier), pp. 50–58.

Xing, H.L., Dong, L., Wang, Z.P., Zhang, H.Y., Han, C.Y., Liu, B., Wang, X.C., and Chen, Q.J. (2014). A CRISPR/Cas9 toolkit for multiplex genome editing in plants. BMC Plant Biol. **14:** 327.

Zhang, X. (2017). Biogeochemistry: A plan for efficient use of nitrogen fertilizers. Nature **543:** 322–323.

Zhang, Y., Liang, W., Shi, J., Xu, J., and Zhang, D. (2013). *MYB56* encoding a R2R3 MYB transcription factor regulates seed size in *Arabidopsis thaliana.* J. Integr. Plant Biol. **55:** 1166–1178.

Zhao, S., Zhang, M.L., Ma, T.L., and Wang, Y. (2016). Phosphorylation of ARF2 relieves its repression of transcription of the K^+ transporter gene *HAK5* in response to low potassium stress. Plant Cell **28:** 3005–3019.

Zhong, R., Lee, C., Zhou, J., McCarthy, R.L., and Ye, Z.H. (2008). A battery of transcription factors involved in the regulation of secondary cell wall biosynthesis in *Arabidopsis.* Plant Cell **20:** 2763–2782.

Zhou, J., Lee, C., Zhong, R., and Ye, Z.H. (2009). MYB58 and MYB63 are transcriptional activators of the lignin biosynthetic pathway during secondary cell wall formation in *Arabidopsis.* Plant Cell **21:** 248–266.

Zörb, C., Senbayram, M., and Peiter, E. (2014). Potassium in agriculture--status and perspectives. J. Plant Physiol. **171:** 656–669.